Effect of Biodeterioration on Modeling Parameters of Code-Compliant Cross-Laminated Timber Lateral Connections

Ian Morrell
Kenneth E. Udele
Jeffrey J. Morrell
Arijit Sinha

Abstract

The effect of biodeterioration on the structural connection performance of timber for conventional framing and mass timber has been investigated recently, but there is a need for additional data as well as for the development of analytical models to utilize these data. An empirical material model (seismic analysis of wood frame shear walls) was fitted to cyclic connection test data of four species of cross-laminated timber at different levels of biodeterioration by two brown-rot fungi. These model inputs were then analyzed to account for trends between wood species and fungal species. Weak trends were most prominent for initial stiffness, intercept load, and displacement at peak force. Correlations were poor with postyield and postpeak stiffness modifiers. These relationships were consistent both as a function of time and as a function of mass loss, but additional data are needed to more accurately predict the effects. The limited relationships likely reflect the variations in fungal decay across the test members.

One of the most used materials in the shift to mass timber construction has been cross-laminated timber (CLT). Substantial research has gone into structural characterization and design with CLT, ranging from floors, diaphragms (Popovski et al. 2016; Beairsto et al. 2022; Line et al. 2022a, 2022b), shear walls (Gavric et al. 2015; Popovski and Gavric 2016; Ho et al. 2017; Amini et al. 2018, 2021; van de Lindt et al. 2019; Moerman et al. 2023), and connections for the aforementioned elements. However, there are other concerns that can affect the structural integrity of the structure. Especially important are considerations relating to the risk of moisture accumulation that create conditions conducive to biodeterioration leading to losses in material properties of wood (Wang et al. 2018, Cappellazzi et al. 2020, Udele et al. 2021, Ayanleye et al. 2022). CLT is not immune from moisture intrusion and subsequent decay and could be subject to similar issues. Despite best intentions and efforts, some structures will be affected by moisture, and both the direct moisture effects, such as dimensional changes, and indirect effects, such as biodeterioration, need to be understood.

Understanding effects of biodeterioration on structural performance of CLT is critical, especially in load-bearing panels, but to date relatively few studies have examined the effects of decay on structural performance of building assemblies. To address this gap, Sinha et al. (2020) proposed a method to characterize biological degradation in building assemblies, especially connection systems. Udele et al. (2023) used this method to investigate wall-to-floor CLT connections after exposure to two brown-rot fungi for up to 40 weeks. Significant reductions in load-carrying and energy dissipation capacity were observed at the end of the exposure time, with a 74 to 90 percent reduction in energy dissipation in some assemblies. Yermán et al. (2022) showed that ultimate strength of nailed timber connections decreased by 40 to 60 percent after 34 weeks of exposure to brown- and white-rot fungi, but noted no significant change

The authors are, respectively, Postdoctoral Scholar, Postdoctoral Scholar, Distinguished Professor Emeritus, and Professor and JELD-WEN Chair in Wood-Based Composites Sci., Wood Sci. and Engineering, Oregon State Univ., Corvallis (ian.morrell@oregonstate.edu [corresponding author], Kenneth.udele@oregonstate.edu, jeff.morrell@oregonstate.edu, arijit.sinha@oregonstate.edu). This paper was received for publication in December 2023. Article no. 23-00064.

Forest Prod. J. 74(2):130–142.
doi:10.13073/FPJ-D-23-00064

in stiffness. Kent et al. (2005) reported similar observations for nailed connections of oriented strand board to Douglas-fir exposed to brown-rot fungi for up to 30 weeks; a 0.1 change in specific gravity was associated with a 60 percent drop in energy dissipation of the connections but initial stiffness was not significantly affected.

Engineering models are useful for analyzing connections (Shen et al. 2013, Mahdavifar et al. 2019, Bhandari et al. 2023) and incorporating data from experimental investigations of connections into larger models. One common engineering model for wood lateral systems is the seismic analysis of wood frame shear walls (SAWS) model (Folz and Filiatrault 2004), which is a 10-parameter model, with five parameters modeling the envelope of the response and five parameters defining cyclic unloading, reloading, and degradation behaviors. The SAWS material model is implemented within OpenSees (McKenna et al. 2010) and was originally developed for conventional framed wood shear walls. As both conventional framed wood shear walls and most mass timber connections are heavily reliant on the behavior of small-diameter metal dowels, typically nails and screws, for their structural response, this model has been used for different mass timber connections (Shen et al. 2013, Mahdavifar et al. 2019, Mahr et al. 2020, Miyamoto et al. 2020, Bora et al. 2021). The envelope curve of the SAWS model has been used to model the effects of environmental changes on CLT connections both for elevated temperature (Mahr et al. 2020) and water intrusion (Bora et al. 2021). This suggests that the model could be useful for determining changes in hysteretic properties as a function of exposure to environmental effects.

Objectives

Understanding the effects of fungal biodeterioration on structural performance of mass timber connections is vital for ensuring the most effective application of these systems. Especially important is assisting designers in assessing and determining required repairs for existing structures affected by biodeterioration. The ability to effectively model the structural effects of biodeterioration can assist practitioners in both the design and analysis of mass timber structures. Therefore, the objectives of this study were to (1) develop model parameters for a common connection model (SAWS) from hysteretic results of a biodeterioration study (Udele et al. 2023); (2) investigate changes in the above parameters as a function of exposure time and mass loss; and (3) compare these trends across four CLT species exposed to two brown-rot fungi.

Materials and Methods

Experimental methods

Two CLT blocks were connected to form a T-shaped assembly using the A3 floor-to-wall connection developed by Amini et al. (2018) and van de Lindt et al. (2022), which was included in the 2021 special design provisions for wind and seismic design (AWC 2022). This connection used a bent 12-gauge (2.7 mm), A653 grade 33 galvanized steel plate (ASTM 2020) connected to the wall element using eight 8d common nails and to the floor element using two 16-mm bolts (Fig. 1). Each test specimen included two floor-to-wall connectors to avoid eccentricity.

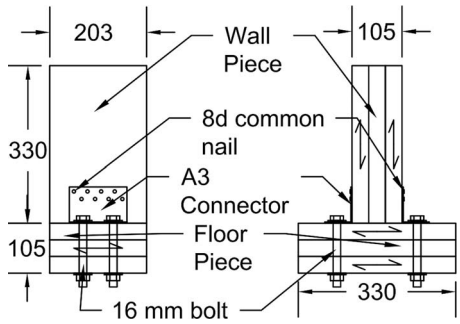

Figure 1.—Specimen layout (all dimensions mm).

A total of four CLT types was tested: V1 (Douglas-fir), V2 (spruce–pine–fir), V3 (southern pine), and CV3M1 (Norway spruce; APA 2018). All CLT pieces in this study were three ply, with 35-mm-thick plies for a total thickness of 105 mm. The two brown-rot species investigated were *Rhodonia placenta* and *Gloeophyllum trabeum*. Initial moisture contents were checked using a 50-mm pin-type probe attached to a Delmhorst RDM3 moisture meter to ensure blocks were approximately 12 $\pm$ 3 percent, per ANSI/APA PRG-320 (APA 2018). Since the aim of the study was to mainly characterize the performance of the connections, the pins were used to take moisture readings at three different locations around the A3 connectors to account for moisture variations. The CLT specimens were fully immersed in water for 4 weeks before inoculation to create conditions suitable for fungal growth and selected assemblies were periodically weighed to determine moisture uptake. Initial and final masses of the assemblies were used to determine moisture gain over the 4 weeks of soaking. Specimens were sterilized to avoid cross-contamination, and consequently inoculated with either of the brown-rot fungi. Sterilization was done in a Wellons kiln drier with temperatures set at 75°C for up to 14 hours. This method was sufficient to raise and hold the core of the CLT assemblies to a temperature of 70°C for up to 2 hours. The specimens were inoculated with fungal-colonized grain and placed in closed containers that were stored in a climate-controlled room at 27°C to accelerate fungal growth. Samples were harvested after 10, 20, 30, and 40 weeks. Exterior fungal growth was removed from harvested specimens and the specimens were air-dried before testing.

Dry controls and wet controls with no fungus were tested for comparison. Dry controls were specimens tested as made, whereas wet controls were soaked until moisture levels exceeded fiber saturation point, dried, and then tested. The purpose of these two treatment groups was to separate moisture-induced changes from fungal degradation. The wet controls were treated as exposure week 0 for both fungi. A total of 10 specimens was evaluated per test series (Table 1).

Testing was conducted using a 178-kN universal testing machine (Fig. 2). The specimens were tested quasistatically following the basic abbreviated CUREE protocol (Krawinkler et al. 2001) using ASTM E2126 (ASTM 2019) as a guide. The reference displacement for this, from previous testing by Bora et al. (2021), was 12.7 mm, and testing was conducted at a cyclic rate of 0.08 Hz. The displacement protocol included cycles with amplitudes through three times the

Table 1.—Testing matrix.

Factors	Description	Quantity
Wood species	Douglas-fir	4
	Norway spruce	
	Spruce–pine–fir	
	Southern pine	
Fungi	*Gloeophyllum trabeum*	2
	Rhodonia placenta	
Exposure time	0 dry, 0 wet, 10, 20, 30, 40 wk	6
Number of replicates		10
Total		480

reference displacement. Testing was concluded when one of the following occurred: all nails in the connection had fractured or fully withdrawn, complete delamination occurred between any of the plies in the wall piece, or the conclusion of the displacement protocol. Instrumentation included the actuator linear variable differential transformer to measure displacement and for feedback control and the actuator load cell for force measurement.

SAWS analysis

Load and displacement data were used to visualize hysteresis plots (Fig. 3a). The hysteretic plot was used to generate an envelope or a backbone curve by finding the peak force and corresponding displacement in each primary cycle of the CUREE displacement protocol. The hysteretic data

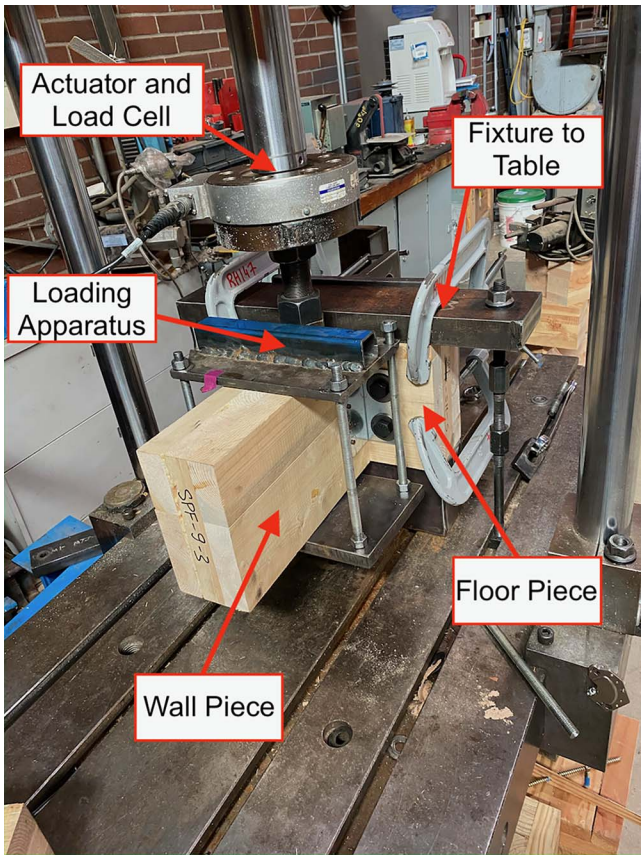

Figure 2.—Physical testing apparatus.

can be used with different engineering models to analyze the response and observe trends. These engineering models can also be used in design by practitioners. Although the SAWS model involves 10 parameters, some of these parameters are esoteric and harder to derive and compare. As a result, only the parameters defining the envelope of the response were used in this study. These parameters were F_0, the y-intercept of the postyield stiffness line, D_u, the displacement at peak force, S_0, the initial stiffness, R_1, the ratio of the postyield stiffness to the initial stiffness, and R_2, the ratio of the postpeak stiffness to the initial stiffness (Fig 3b).

These parameters were used to model the force at a given displacement before peak force using Equation 1 from Dolan and Madsen (1992) and Folz and Filiatrault (2001), whereas postpeak response is given by Equation 2 from Folz and Filiatrault (2001):

$$F_\Delta = (F_0 + R_1 S_0 \Delta)\left(1 - e^{\left[-\frac{S_0 \Delta}{F_0}\right]}\right) \text{ for } \Delta \le D_u \quad (1)$$

$$F_\Delta = F_{max} + R_2 S_0 (\Delta - D_u) \text{ for } \Delta > D_u \quad (2)$$

where F_Δ is the force at a given displacement Δ and F_{max} is the force when evaluating Equation 1 at $\Delta = D_u$.

Previous studies have used this methodology for examining mass timber (Mahdavifar et al. 2019, Mahr et al. 2020, Miyamoto et al. 2020, Bora et al. 2021). Similar to this study, both Mahr et al. (2020) and Bora et al. (2021) only looked at the characteristics from the envelope. The last five parameters (R_3, R_4, F_1, alpha, and beta) apply only to the unloading and reloading branches of the hysteretic behavior until the response rejoins the backbone.

The modeling parameters were fitted using the simulated annealing optimization strategy from Matlab (Mathworks Inc. 2017). The primary objective of the optimization strategy is to minimize the percent difference in energy between the experimental and modeled results. Two parameters were taken directly from the data to simplify analysis, D_u and F_{max}. These two parameters were used to define a third parameter in terms of the others using Equation 3:

$$F_0 = F_{max} - R_1 S_0 D_u \quad (3)$$

This simplification meant that only three parameters (S_0, R_1, and R_2) needed to be optimized.

A maximum of 10,000 iterations was conducted on each specimen. The optimization was ended early if the objective function reached a value <2 percent; this occurred for most specimens.

Parameters extracted from each curve were used to calculate the mean, standard deviation, and covariance matrix for each parameter or set of parameters within a test series. These values were then regressed against fungal exposure time.

Results

Salient SAWS results

Detailed analyses of the hysteretic response including maximum force, stiffness, and ductility were presented in Udele et al. (2023). Regression analysis and pairwise comparisons of all these parameters were based on CLT species,

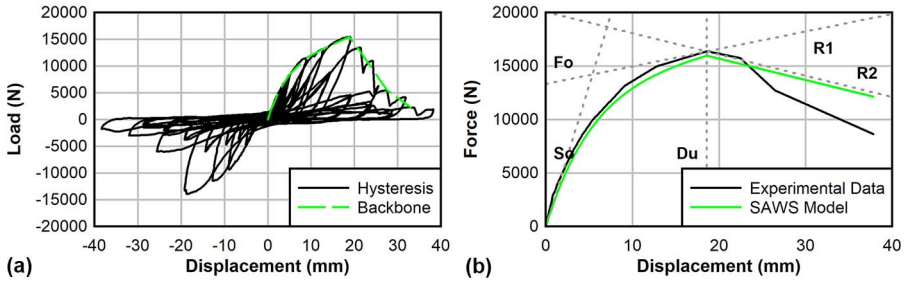

Figure 3.—(a) Backbone from test data and (b) seismic analysis of wood frame shear walls (SAWS) envelope parameters.

inoculation time, and fungus species. Herein, only modeling parameters and their degradation with time or mass loss were investigated (Table 2) and representative experimental and optimized curves can be seen in Figure 4. It is important to note that the SAWS parameters do not allow for an offset at zero force. Some of the later tests exhibited a small slack behavior before picking up force. This was not due to the test fixture, but rather due to slack that developed within the connection itself as a result of deformation from wetting and fungal exposure. These results were not removed from the data, which reduced the fitness of the SAWS model for these samples, as evidenced by the lower values and higher variations for S_0 and F_0. Values tended to decrease as a function of time for the three primary parameters (F_0, D_u, and S_0),

Table 2.—Seismic analysis of wood frame shear walls parameters associated with exposure of cross-laminated timber of different species to wetting and fungal attack over time.

Wood species	Fungus	Exposure time (weeks)	F_0		D_u		S_0		R_1		R_2	
			Mean (N)	COV[a] (%)	Mean (mm)	COV (%)	Mean (N/mm)	COV (%)	Mean	COV (%)	Mean	COV (%)
Douglas-fir	Dry control		13,024	23.0	18.7	15.9	2,811	28.9	0.075	126.2	−0.185	−49.2
	Wet control		9,993	21.0	25.8	8.2	1,530	19.0	0.186	40.9	−0.296	−117.1
	Gloeophyllum trabeum	10	10,127	50.1	18.8	22.5	1,903	19.7	0.201	102.5	−0.738	−200.6
		20	6,173	60.1	17.9	40.8	1,521	12.3	0.366	56.3	−0.261	−135.8
		30	7,036	64.6	17.7	30.7	1,532	24.3	0.356	75.7	−1.323	−195.7
		40	4,935	64.8	15.2	26.5	1,460	22.1	0.367	47.1	−0.590	−124.6
	Rhodonia placenta	10	9,686	53.0	18.6	35.3	1,904	24.8	0.213	88.6	−0.152	−36.6
		20	6,618	61.5	16.4	34.7	1,513	27.1	0.306	72.2	−0.222	−72.1
		30	7,277	65.9	17.1	55.3	1,624	32.8	0.181	128.1	−0.283	−99.9
		40	3,300	76.9	13.4	35.9	1,159	30.9	0.349	60.0	−0.245	−161.5
Norway spruce	Dry control		8,809	39.0	18.7	2.1	2,130	37.5	0.171	79.9	−0.217	−41.1
	Wet control		9,824	32.7	27.5	11.1	1,409	11.8	0.163	66.1	−0.309	−59.2
	G. trabeum	10	8,139	61.9	20.4	28.3	1,607	24.1	0.263	80.5	−0.279	−108.9
		20	5,535	78.2	15.9	34.4	1,638	22.4	0.356	62.0	−0.142	−42.8
		30	9,466	46.1	27.3	36.2	1,359	28.6	0.171	100.7	−0.218	−55.9
		40	7,246	67.5	18.7	42.6	1,198	32.4	0.299	89.6	−0.152	−48.6
	R. placenta	10	9,413	43.0	19.5	36.4	1,688	31.9	0.153	111.4	−0.601	−181.6
		20	3,620	82.9	15.6	39.9	1,213	15.0	0.443	57.9	−0.188	−55.5
		30	6,788	73.6	24.1	40.3	983	39.0	0.105	151.1	−0.231	−58.9
		40	3,800	77.6	11.4	33.9	1,119	29.5	0.401	89.8	−0.145	−51.5
Spruce–pine–fir	Dry control		9,104	35.2	19.9	13.3	2,033	54.5	0.170	124.2	−0.271	−92.6
	Wet control		10,938	25.5	27.6	12.3	1,366	17.4	0.111	86.3	−0.308	−51.6
	G. trabeum	10	9,637	43.1	22.0	14.0	1,535	30.9	0.155	92.3	−2.082	−138.6
		20	13,027	24.9	22.2	27.2	2,015	28.9	0.039	124.0	−0.879	−161.6
		30	9,395	58.0	22.8	30.5	1,486	30.4	0.195	108.6	−0.221	−80.3
		40	4,836	76.5	18.8	37.1	1,249	27.2	0.411	64.4	−0.162	−37.2
	R. placenta	10	9,795	44.2	19.9	19.7	1,858	27.9	0.153	116.5	−0.379	−101.6
		20	6,628	60.2	16.9	41.2	1,296	37.0	0.253	92.8	−0.189	−54.3
		30	7,667	43.8	19.3	17.6	1,363	32.2	0.133	88.0	−0.165	−38.6
		40	8,913	49.8	23.1	30.7	1,354	39.1	0.187	107.3	−0.204	−72.0
Southern pine	Dry control		12,070	27.7	21.0	15.6	2,494	37.8	0.076	106.0	−0.390	−152.0
	Wet control		7,626	61.3	26.2	7.5	1,247	26.9	0.283	72.3	−0.228	−60.4
	G. trabeum	10	9,121	64.6	21.6	35.5	1,737	27.6	0.250	110.1	−0.151	−35.0
		20	8,438	57.8	17.4	35.3	1,657	21.6	0.202	108.2	−0.133	−38.4
		30	3,832	49.9	16.4	30.6	1,026	22.3	0.436	51.5	−0.142	−46.4
		40	5,783	74.6	16.2	50.3	1,149	48.3	0.330	85.1	−0.282	−127.5
	R. placenta	10	6,373	70.7	18.1	20.3	1,558	26.5	0.401	70.3	−0.155	−76.1
		20	5,056	101.0	13.7	52.5	1,225	19.5	0.377	84.3	−0.153	−35.4
		30	4,940	96.2	20.0	33.0	9,61	36.7	0.419	94.2	−0.168	−46.7
		40	4,794	67.6	12.0	26.4	1,005	35.8	0.293	94.4	−0.158	−50.7

[a] COV = coefficient of variation.

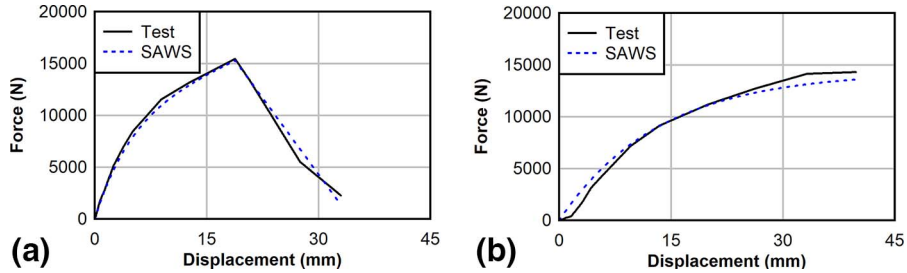

Figure 4.—Representative seismic analysis of wood frame shear walls (SAWS) and hysteretic backbone curves for (a) a Douglas-fir sample exposed to Gloeophyllum trabeum for 10 weeks; (b) a spruce–pine–fir sample exposed to Rhodonia placenta for 40 weeks.

but discrepancies were observed within these parameters where the property seemingly increased. These discrepancies were attributed to the high variance inherent in biological durability testing (Kent et al. 2005, Yermán et al. 2022). The fungi were introduced from the exterior surface of the assemblies and were likely to differentially colonize the wood, creating differing degrees of damage.

Linear regressions through both time and mass loss can be used to elucidate relationships between the SAWS parameters and the degree of degradation using degradation as a function of exposure time or as a function of percent mass loss. Although there was some variation between the wood species, in general they all experienced similar trends of direction, magnitude, and model fitness. As such, only one of the wood species, Douglas-fir, will be discussed in detail, and the regressions for all four species can be seen in Tables 3–6.

Both decay fungi show similar losses in the postyield intercept, F_0, as a function of time, with the property reducing in value while increasing in variance as time progressed (Fig. 5). The linear fits through these data were weak, with R^2 of 0.19 and 0.25 for *G. trabeum* and *R. placenta*, respectively. Fungal attack varies with moisture content, wood chemistry, wood anatomy, and wood grain orientation, among other factors. The large scale of the test assembly, compared with typical tests of fungal degradation, further increases the potential for differing degrees of decay in different areas of the same specimen. Larger differences were observed as a function of percent mass loss, with *R. placenta* exhibiting a slower degradation. Both of these fungi are widely used in decay tests because they are easily cultured and produced consistent mass losses; however, they are found in different niches. *G. trabeum* tends to be more prevalent in aboveground applications such as windows or door frames where moisture levels tend to be lower and more variable (Duncan and Lombard 1965). *R. placenta* is found in a variety of applications but is a common invader of Douglas-fir heartwood (Smith et al. 1987). *R. placenta* reduced the mass of the specimens at a faster rate with respect to time, but these losses had less impact on F_0 than *G. trabeum*. Fitting changes in F_0 as a function of mass loss

Table 3.—Linear regressions for Douglas-fir seismic analysis of wood frame shear walls (SAWS) parameters as functions of either exposure time or percent mass loss.

Species	Fungus	SAWS parameter	Fungus		
			Slope	Intercept	R^2
		Regression as a function of time (weeks)			
Douglas-fir	*Gloeophyllum trabeum*	F_0	−132.1	10,294	0.20
		D_u	−0.22	23.52	0.28
		S_0	−5.1	1,691.5	0.05
		R_1	0.005	0.192	0.13
		R_2	−0.012	−0.407	0.01
	Rhodonia placenta	F_0	−157.9	10,534	0.25
		D_u	−0.26	23.52	0.27
		S_0	−10.2	1,750.4	0.10
		R_1	0.003	0.188	0.05
		R_2	0.000	−0.234	0.00
		Regression as a function of mass loss (%)			
Douglas-fir	*G. trabeum*	F_0	−432.6	9,955	0.14
		D_u	−0.68	22.70	0.18
		S_0	−24.2	1,718.2	0.07
		R_1	0.020	0.190	0.13
		R_2	−0.057	−0.336	0.02
	R. placenta	F_0	−306.1	10,124	0.21
		D_u	−0.62	23.78	0.32
		S_0	−23.5	1,757.0	0.11
		R_1	0.001	0.236	0.00
		R_2	0.006	−0.297	0.02

Table 4.—Linear regressions for Norway spruce seismic analysis of wood frame shear walls (SAWS) parameters as functions of either exposure time or percent mass loss.

Species	Fungus	SAWS parameter	Regression parameters		
			Slope	Intercept	R^2
		Regression as a function of time (weeks)			
Norway spruce	*Gloeophyllum trabeum*	F_0	−38.3	8808	0.01
		D_u	−0.11	24.10	0.04
		S_0	−6.7	1,576.4	0.07
		R_1	0.002	0.214	0.02
		R_2	0.004	−0.295	0.09
	Rhodonia placenta	F_0	−146.8	9,623.9	0.22
		D_u	−0.28	25.16	0.22
		S_0	−12.9	1539.7	0.20
		R_1	0.004	0.167	0.06
		R_2	0.007	−0.434	0.04
		Regression as a function of mass loss (%)			
Norway spruce	*G. trabeum*	F_0	−169.4	9525	0.05
		D_u	−0.26	24.27	0.04
		S_0	−21.2	1628.2	0.11
		R_1	0.007	0.187	0.04
		R_2	0.005	−0.260	0.02
	R. placenta	F_0	−282.6	9,826	0.19
		D_u	−0.36	23.61	0.08
		S_0	−26.5	1,577.3	0.19
		R_1	0.003	0.225	0.00
		R_2	0.004	−0.334	0.00

exhibited weaker trends for both fungi when compared with exposure time.

One SAWS parameter that showed higher causality was ultimate displacement, D_u (Fig 6). Displacement capacity decreased as a function of exposure time for both fungi, with the average D_u dropping approximately 40 percent over 40 weeks or a linear rate of approximately 0.2 mm of displacement capacity a week. There were weak but suggestive coefficients of determination at 0.27 and 0.28 for *G. trabeum* and *R. placenta*, respectively. Similar trends were seen between F_0 and D_u with respect to percent mass loss, with *R. placenta* associated with slower degradation than *G. trabeum*.

Table 5.—Linear regressions for spruce–pine–fir seismic analysis of wood frame shear walls (SAWS) parameters as functions of either exposure time or percent mass loss.

Species	Fungus	SAWS parameter	Regression parameters		
			Slope	Intercept	R^2
		Regression as a function of time (weeks)			
Spruce–pine–fir	*Gloeophyllum trabeum*	F_0	−124.4	12,055	0.14
		D_u	−0.17	26.01	0.16
		S_0	−2.8	1,586.9	0.01
		R_1	0.006	0.054	0.19
		R_2	0.022	−1.161	0.04
	Rhodonia placenta	F_0	−61.8	10,023	0.05
		D_u	−0.09	23.24	0.05
		S_0	−5.2	1,551.4	0.02
		R_1	0.001	0.141	0.01
		R_2	0.004	−0.333	0.08
		Regression as a function of mass loss (%)			
Spruce–pine–fir	*G. trabeum*	F_0	−281.4	11,722	0.08
		D_u	−0.53	26.74	0.17
		S_0	−4.6	1,565.5	0.00
		R_1	0.015	0.066	0.12
		R_2	0.020	−0.887	0.00
	R. placenta	F_0	−275.2	11,438	0.16
		D_u	−0.58	26.93	0.28
		S_0	−13.8	1,580.5	0.03
		R_1	0.004	0.131	0.02
		R_2	0.010	−0.342	0.07

Table 6.—Linear regressions for southern yellow pine seismic analysis of wood frame shear walls (SAWS) parameters as functions of either exposure time or percent mass loss.

Species	Fungus	SAWS parameter	Regression parameters		
			Slope	Intercept	R^2
		Regression as a function of time (weeks)			
Southern yellow pine	*Gloeophyllum trabeum*	F_0	−89.7	8,754.9	0.07
		D_u	−0.25	24.61	0.26
		S_0	−9.1	1,544.9	0.07
		R_1	0.003	0.245	0.03
		R_2	−0.001	−0.168	0.01
	Rhodonia placenta	F_0	−71.0	7,177.1	0.05
		D_u	−0.26	23.31	0.30
		S_0	−10.8	1,415.5	0.15
		R_1	0.000	0.347	0.00
		R_2	0.001	−0.198	0.03
		Regression as a function of mass loss (%)			
Southern yellow pine	*G. trabeum*	F_0	−164.7	8,382	0.04
		D_u	−0.62	24.92	0.25
		S_0	−8.7	1,437.9	0.01
		R_1	0.003	0.272	0.01
		R_2	−0.001	−0.175	0.00
	R. placenta	F_0	−296.1	8,786	0.20
		D_u	−0.67	24.867	0.42
		S_0	−27.6	1,481.7	0.22
		R_1	0.009	0.266	0.04
		R_2	0.004	−0.213	0.07

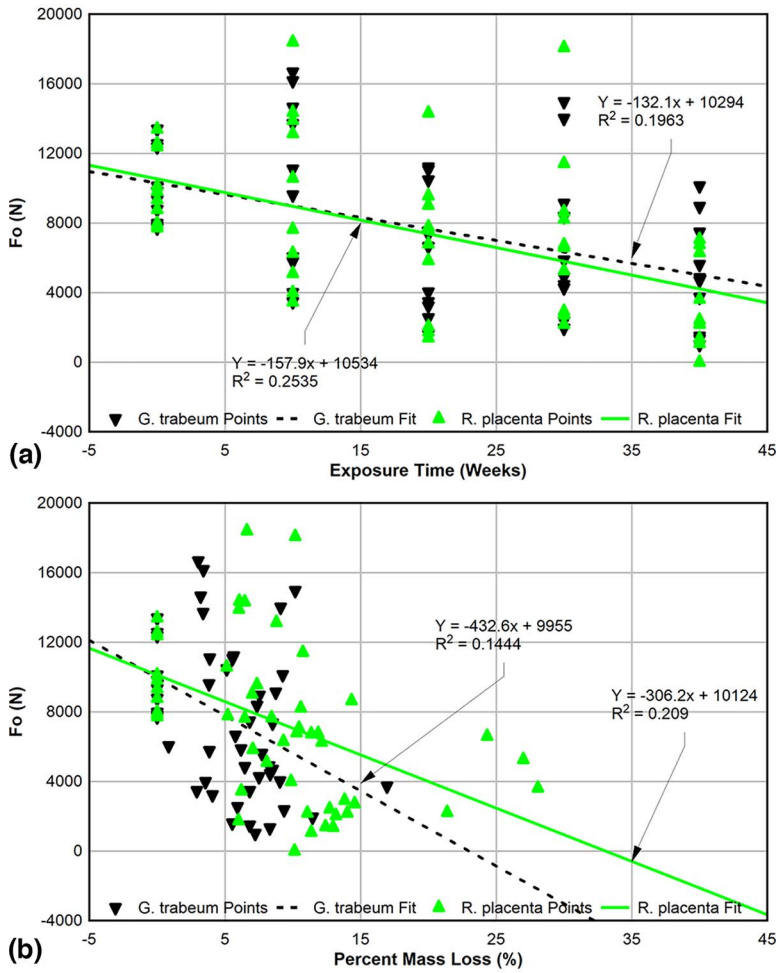

Figure 5.—Seismic analysis of wood frame shear walls parameter distribution of F_0 as a function of (a) time and (b) percent mass loss after exposure of Douglas-fir samples to Gloeophyllum trabeum or Rhodonia placenta.

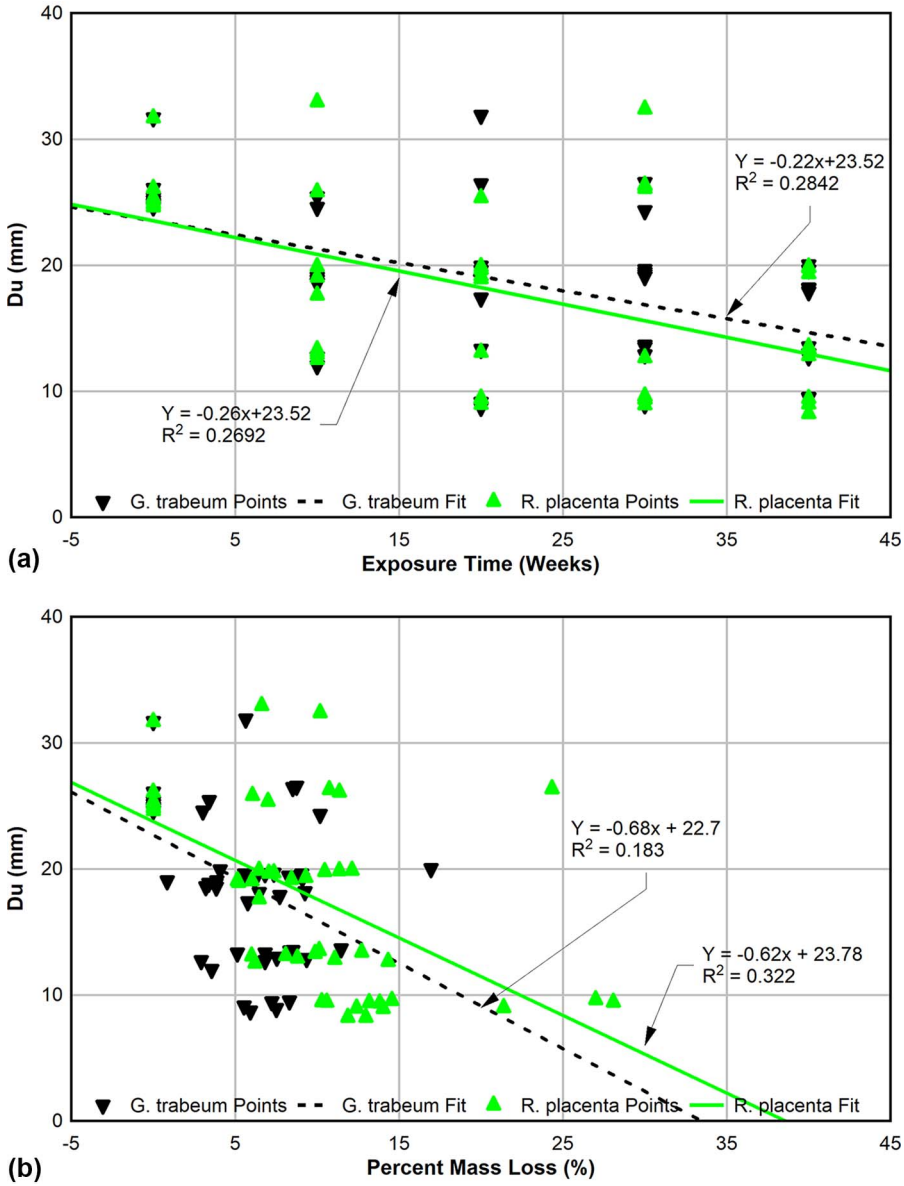

Figure 6.—Seismic analysis of wood frame shear walls parameter distribution of D_u as a function of (a) time and (b) percent mass loss for Douglas-fir samples after exposure to Gloeophyllum trabeum or Rhodonia placenta.

The initial stiffness term, S_0, showed little change with respect to either exposure time or mass loss (Fig. 7). Stiffness tended to be similar for the first 30 weeks of exposure; it decreased and became more variable at 40 weeks for both fungi. Assemblies exposed to *R. placenta* exhibited higher, more variable stiffness losses at 40 weeks. R^2 values for both exposure time and mass loss were low for both fungi. Fungal degradation is rarely uniform across a member and this characteristic would tend to induce variable impacts on stiffness for individual elements. Eventually, this variability would decline as the decay process progressed.

As with the other parameters, R_1, the ratio between postyield and initial stiffness, became more variable with time and mass loss, reflecting the inherent variability of biological activity; however, the general trend was positive for both decay fungi (Fig. 8). This positive trend did not suggest that stiffness increased as a function of exposure time or percent mass loss, since initial and postyield stiffness both declined. Postyield stiffness decreases more slowly than initial stiffness, thereby increasing the ratio as a function of time or increased mass loss. Despite some evidence of trends, the high variability once again resulted in low correlations for this parameter.

There was little correlation between the ratio of postpeak to initial stiffness (R_2) and exposure time or percent mass loss for either fungus (Fig. 9). These poor correlations reflect the lack of consistent failure paths for each connection. Failures were generally dependent on local nail failures and these varied widely between assemblies as a result of differing degrees of decay. Additionally, some of the later tests had to be terminated because of wood failure away from the connection due to degradation. These failures sometimes occurred before a postpeak behavior was observed, further increasing variability.

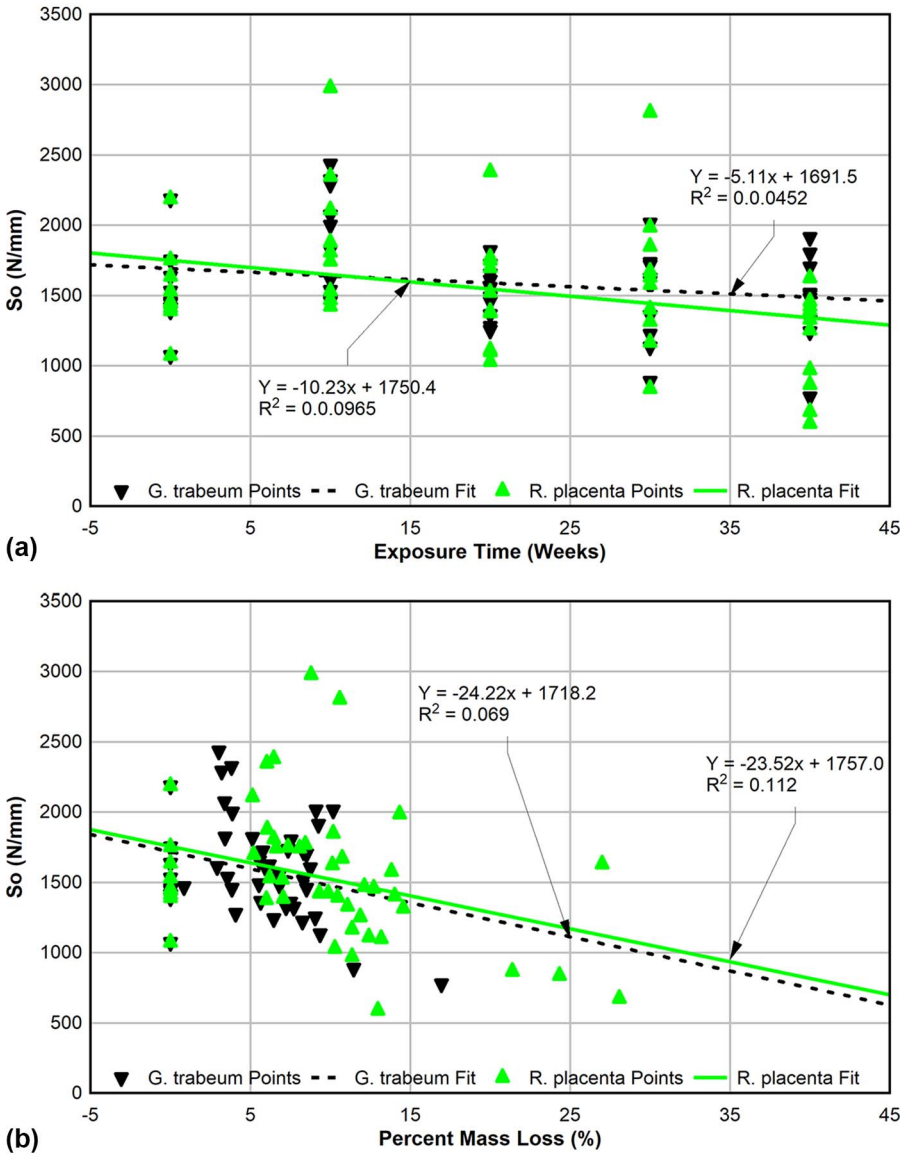

Figure 7.—Seismic analysis of wood frame shear walls parameter distribution of S_0 as a function of (a) time and (b) percent mass loss for Douglas-fir samples after exposure to Gloeophyllum trabeum or Rhodonia placenta.

Discussion

Although the variable nature of the decay process resulted in poor correlations between fungal attack and the SAWS parameters, there were some consistent trends. Three parameters (F_0, D_u, and S_0) generally decreased as a function of time. The postyield stiffness modifier, R_1, showed that postyield stiffness, R_1S_0, decreased as a function of exposure time, but at a slower rate than initial stiffness, S_0, alone. Postpeak stiffness, R_2, showed no observable trends as a function of exposure. Part of the lack of observable trends in R_2 may be due to premature failure of pieces at higher exposure times, resulting in less available data for the regression. Property losses were consistently seen between the dry and wet controls, with the wet controls having higher ultimate displacement capacity, D_u, but lower initial, S_0, and postyield stiffness, R_1S_0. These results contrast with those of Bora et al. (2021), who found little difference between dry control and redried specimens. Differences in the drying protocol may help explain the results since Bora et al. (2021) air dried the specimens, whereas the specimens in this study were dried using a kiln at a slow drying rate.

Ultimately, none of the regressions through the properties as functions of either time or mass loss accurately determined biodeterioration-associated loss of connection properties. Decay is rarely uniform in a timber assembly and the scale of these test members made it highly likely that there would be considerable variation in the degree of decay. As a result, the degree of decay close to the connection could vary considerably between assemblies even if the average mass losses were similar. This likely contributed to the very high variance.

Another observation with the data was a flat or weak slightly positive trend for R_1. This trend indicated that postyield stiffness losses occurred at the same or slower rate

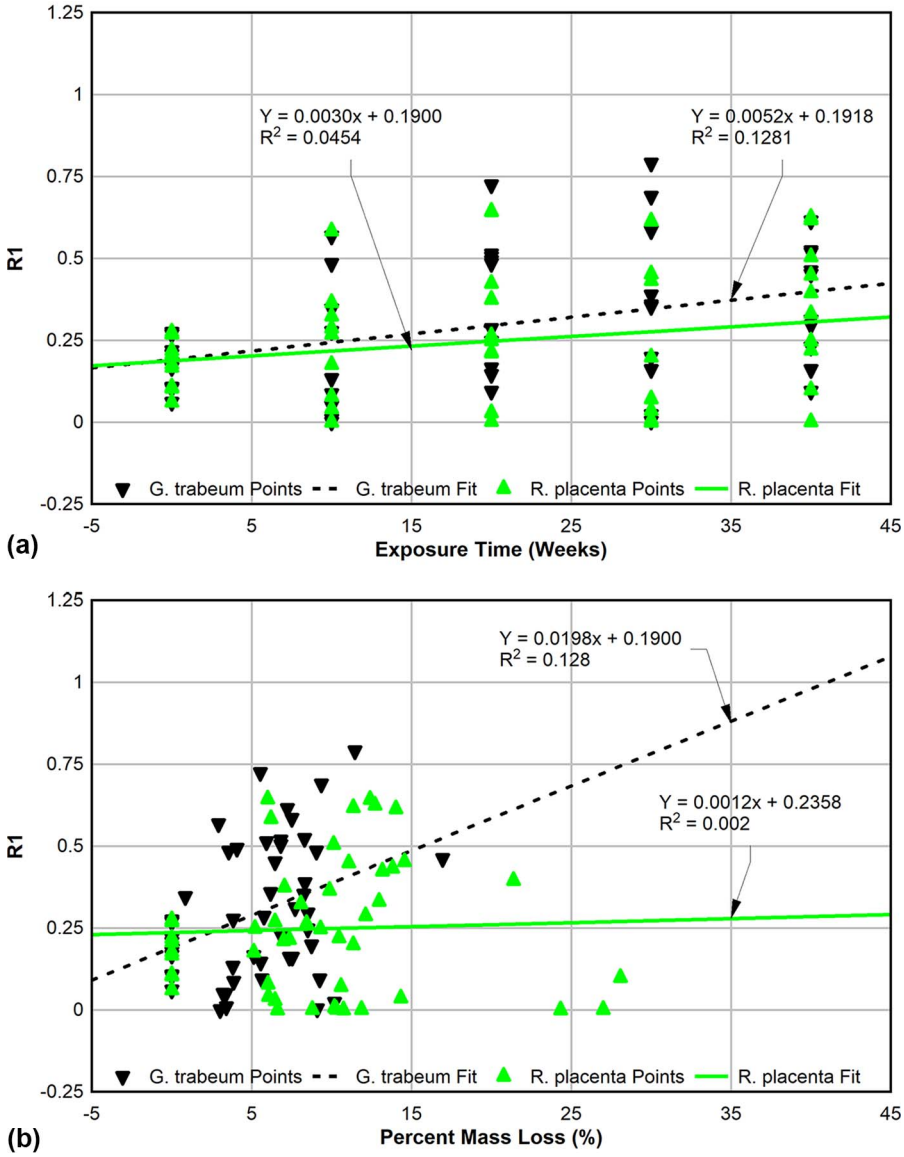

Figure 8.—Seismic analysis of wood frame shear walls parameter distribution of R_1 as a function of (a) time and (b) percent mass loss for Douglas-fir samples after exposure to Gloeophyllum trabeum or Rhodonia placenta.

than those for S_0. Thus, although there were postyield stiffness losses, they occurred more slowly than losses in initial stiffness. This contrasts with previous work on wetting effects that showed no obvious trend in R_1 with prolonged wetting (Bora et al. 2021). This suggests that the effects of biodeterioration on postyield stiffness are unrelated to the moisture trend. Additionally, R_2 showed no appreciable trend as a function of time or mass loss, suggesting that postpeak stiffness does not have a trend outside of the initial S_0 losses. This finding on R_2 lines up with the moisture trend in Bora et al. (2021), suggesting that, outside of damage causing more variation in the postpeak performance, no appreciable trend can be found in the postpeak stiffness.

One important factor in any study involving biodeterioration is the organisms involved. In this study, two brown-rot fungi were used. Brown-rot fungi generally preferentially use the hemicelluloses and cellulose, leaving a heavily modified residual lignin. However, brown-rot fungi have a range of decay capacities, which can vary depending on the wood species and environmental conditions. In this study, samples exposed to *R. placenta* exhibited higher property losses than those exposed to *G. trabeum* and these differences were also present with mass loss. This suggests that, although the correlation between assembly mass loss and connection properties was weak, mass loss did correlate with structural property losses for larger mass timber connections.

Although the data produced only suggestive conclusions, the application of the SAWS material appears useful for designers. There are limited data on the effect of biodeterioration on connection properties of mass timber and existing data focus primarily on strength and initial stiffness. Quantifying the effects of decay on postyield and postpeak behavior may make it possible to examine the effects of biodeterioration on structures subjected to an earthquake. Although more data

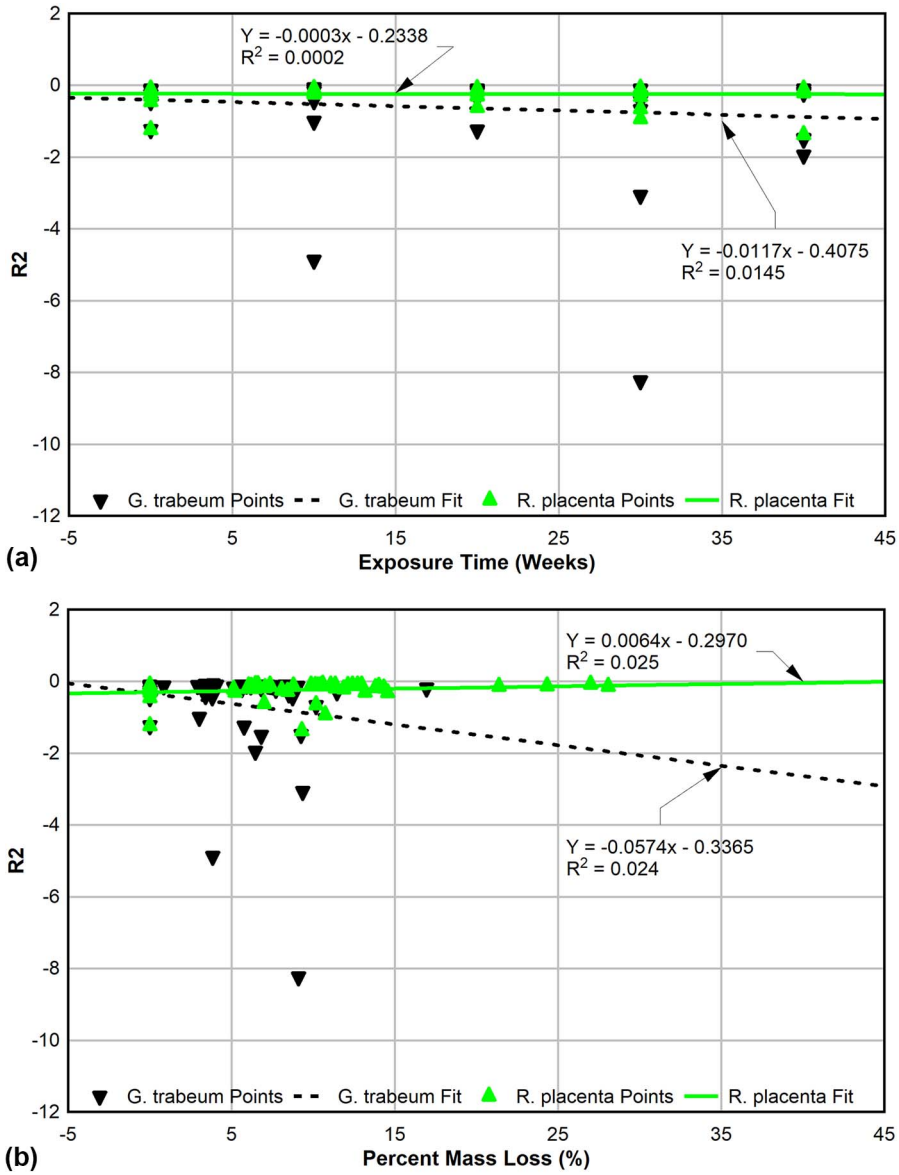

Figure 9.—Seismic analysis of wood frame shear walls parameter distribution of R_2 as a function of (a) time and (b) percent mass loss for Douglas-fir samples after exposure to Gloeophyllum trabeum or Rhodonia placenta.

are needed, fitting degradation data to engineering models appears to be an effective approach.

Conclusions

The SAWS modeling parameters were derived for CLT connection of four species after exposure to two different fungi for a total of 40 weeks. Statistically, the SAWS parameters were generally poorly correlated with fungal-associated mass losses of the CLT assemblies, but there were some trends with some parameters that suggest they could be useful with additional data. Overall, a few conclusions can be made:

1. SAWS parameters can be determined from hysteretic data and the parameters can be used to generally track trends due to biodeterioration.
2. Connection properties were affected by biodeterioration, showing average losses of 13 and 40 percent over 40 weeks of exposure for initial stiffness and ultimate displacement, respectively.
3. The variability of fungal attack and the large dimensions of the assemblies likely created nonuniform decay in the CLT that affected the results. The use of fewer variables (fewer fungi or wood species) and perhaps smaller assemblies would allow for additional replication with more uniform decay.
4. The results suggest that the postyield stiffness reduced at or more slowly than the rate of initial stiffness for all CLT and fungal species.

Future studies into the effects of biodeterioration on connection performance will help to solidify the findings of this study, especially on smaller-scale connections. Additional

research using SAWS parameters and physical testing of full-scale walls would also assist practitioners in the confidence of modeling walls using small-scale deterioration connection data.

Acknowledgments

This research was funded by US Department of Agriculture National Institute of Food and Agriculture Agriculture and Food Research Initiative (grant no. 2018-67021-27718). The authors thank Jed Cappellazzi, Dr. Tyler Deboodt, and Anthony Newton for their technical assistance with experimentation.

Literature Cited

American Wood Council (AWC) 2022. National design specifications for wood construction. AWC, Reston, Virginia.

Amini, M. O., J. W. Van De Lindt, D. Rammer, and S. Pei. 2021. Rocking behavior of high-aspect-ratio cross-laminated timber shear walls: Experimental and numerical investigation. *J. Archit. Eng.*, 27(3):04021013. https://doi.org/10.1061/(ASCE)AE.1943-5568.0000473

Amini, M. O., J. W. van de Lindt, D. Rammer, S. Pei, P. Line, and M. Popovski. 2018. Systematic experimental investigation to support the development of seismic performance factors for cross laminated timber shear wall systems. *Eng. Struct*. 172:392–404. https://doi.org/10.1016/j.engstruct.2018.06.021

APA—The Engineered Wood Association. 2018. Standard for performance-rated cross laminated timber. ANSI/APA PRG 320. Tacoma, Washington.

ASTM International. 2019. Standard test methods for cyclic (reverse) load test for shear resistance of vertical elements of the lateral force resisting systems for buildings. ASTM E2126. ASTM International, West Conshohocken, Pennsylvania.

ASTM International. 2020. Standard specification for steel sheet, zinc-coated (galvanized) or zinc-iron-alloy coated (galannealed) by the hot-dip process. ASTM A653. ASTM International, West Conshohocken, Pennsylvania.

Ayanleye, S., K. Udele, V. Nasir, X. Zhang, and H. Militz. 2022. "Durability and protection of mass timber structures: A review." *Journal of Building Engineering*, 46: 103731. https://doi.org/10.1016/j.jobe.2021.103731.

Beairsto, C., R. Gupta, and T. H. Miller. 2022. Monotonic and cyclic behavior of CLT diaphragms. *Pract. Period. Struct. Des. Constr.* 27(2):04021085. https://doi.org/10.1061/(ASCE)SC.1943-5576.0000658

Bhandari, S., E. C. Fischer, M. Riggio, and L. Muszynski. 2023. Numerical assessment of in-plane behavior of multi-panel CLT shear. *Eng. Struct*. 295. https://doi.org/10.1016/j.engstruct.2023.116846

Bora, S., A. Sinha, and A. R. Barbosa. 2021. Effect of wetting and redrying on performance of cross-laminated timber angle bracket connection. *J. Struct. Eng.* 147(9):04021121. https://doi.org/10.1061/(ASCE)ST.1943-541X.0003074

Cappellazzi, J., M. J. Konkler, A. Sinha, and J. J. Morrell. 2020. Potential for decay in mass timber elements: A review of the risks and identifying possible solutions. *Wood Mater. Sci. Eng*. 15(6):351–360. https://doi.org/10.1080/17480272.2020.1720804

Dolan, J. D. and B. Madsen. 1992. Monotonic and cyclic nail connection tests. *Can. J. Civ. Eng.* 19(1):97–104. https://doi.org/10.1139/l92-010

Duncan, C. G. and F. F. Lombard. 1965. Fungi associated with principal decays in wood products in the United States (Vol. 4). US Department of Agriculture, Washington, D.C.

Folz, B. and A. Filiatrault. 2001. Cyclic analysis of wood shear walls. *J. Struct. Eng.* 127(4):433–441. https://doi.org/10.1061/(ASCE)0733-9445(2001)127:4(433)

Folz, B. and A. Filiatrault. 2004. Seismic analysis of woodframe structures. I: Model formulation. *J. Struct. Eng.* 130(9):1353–1360. https://doi.org/10.1061/(ASCE)0733-9445(2004)130:9(1353)

Gavric, I., M. Fragiacomo, and A. Ceccotti. 2015. Cyclic behavior of CLT wall systems: Experimental tests and analytical prediction models. *J. Struct. Eng.* 141(11):04015034. https://doi.org/10.1061/(ASCE)ST.1943-541X.0001246

Ho, T. X., T. N. Dao, S. Aaleti, J. W. Van De Lindt, and D. R. Rammer. 2017. Hybrid system of unbonded post-tensioned CLT panels and light-frame wood shear walls. *J. Struct. Eng.*, 143(2): 04016171. https://doi.org/10.1061/(ASCE)ST.1943-541X.0001665

Kent, S. M., R. J. Leichti, D. V. Rosowsky, and J. J. Morrell. 2005. Effects of decay on the cyclic properties of nailed connections. *J. Mater. Civ. Eng.* 17(5):579–585. https://doi.org/10.1061/(ASCE)0899-1561(2005)17:5(579)

Krawinkler, H., F. Parisi, L. Ibarra, A. Ayoub, and R. Medina. 2001. Development of a testing protocol for wood frame structures. CUREE-Caltech woodframe project report no. W-02. Stanford University, Palo Alto, California.

Line, P., S. Nyseth, and N. Waltz. 2022a. Full-scale cross-laminated timber diaphragm evaluation. I: Design and full-scale diaphragm testing. *J. Struct. Eng*. 148(5):04022037. https://doi.org/10.1061/(ASCE)ST.1943-541X.0003308

Line, P., S. Nyseth, and N. Waltz. 2022b. Full-scale cross-laminated timber diaphragm evaluation. II: CLT diaphragm connection tests. *J. Struct. Eng*. 148(5):04022038. https://doi.org/10.1061/(ASCE)ST.1943-541X.0003309

Mahdavifar, V., A. R. Barbosa, A. Sinha, L. Muszynski, R. Gupta, and S. E. Pryor. 2019. Hysteretic response of metal connections on hybrid cross-laminated timber panels. *J. Struct. Eng.* 145(1):04018237. https://doi.org/10.1061/(ASCE)ST.1943-541X.0002222

Mahr, K., A. Sinha, and A. R. Barbosa. 2020. Experimental investigation and modeling of thermal effects on a typical cross-laminated timber bracket shear connection. *J. Mater. Civ. Eng.* 32(6):04020111. https://doi.org/10.1061/(ASCE)MT.1943-5533.0003122

Mathworks Inc. (2017). MATLAB Version: 9.3.0 (R2017b). Natick, Massachusetts.

McKenna, F., M. H. Scott, and G. L. Fenves. 2010. "Nonlinear Finite-Element Analysis Software Architecture Using Object Composition." *J. Comput. Civ. Eng.*, 24 (1): 95–107. https://doi.org/10.1061/(ASCE)CP.1943-5487.0000002

Miyamoto, B. T., A. Sinha, and I. Morrell. 2020. Connection performance of mass plywood panels. *Forest Prod. J*. 70(1):12.

Moerman, B., M. Li, T. Smith, and A. Liu. 2023. Cyclic testing of high-capacity CLT shear walls. *J. Struct. Eng.* 149(11):04023148. https://doi.org/10.1061/JSENDH.STENG-12188

Popovski, M., Z. Chen, and B. Gafner. 2016. Structural behaviour of point-supported CLT floor systems. *In:* Proceedings of the World Conference on Timber Engineering, August 22–25, 2016, 9. Vienna, Austria.

Popovski, M. and I. Gavric. 2016. Performance of a 2-Story CLT house subjected to lateral loads. *J. Struct. Eng.* 142(4):E4015006. https://doi.org/10.1061/(ASCE)ST.1943-541X.0001315

Shen, Y., J. Schneider, S. Tesfamariam, S. F. Stiemer, and Z.-G. Mu. 2013. Hysteresis behavior of bracket connection in cross-laminated-timber shear walls. *Constr. Build. Mater*. 48:980–991.

Sinha, A., K. E. Udele, J. Cappellazzi, and J. J. Morrell. 2020. A method to characterize biological degradation of mass timber connections. *Wood Fiber Sci*. 52(4):419–430.

Smith, S. M., R. D. Graham, and J. J. Morrell. 1987. Influence of air-seasoning on fungal colonization and strength properties of Douglas-fir pole sections. *Forest Prod. J*. 37(9):45–48.

Udele, K. E., J. J. Morrell, and A. Sinha. 2021. Biological durability of cross-laminated timber—The state of things. *Forest Prod. J*. 71(2):124–132. https://doi.org/10.13073/FPJ-D-20-00076

Udele, K. E., J. J. Morrell, J. Cappellazzi, and A. Sinha. 2023. Characterizing properties of fungal-decayed cross laminated timber (CLT) connection assemblies. *Constr. Build. Mater*. 409:134080. https://doi.org/10.1016/j.conbuildmat.2023.134080

van de Lindt, J. W., M. O. Amini, D. Rammer, P. Line, S. Pei, and M. Popovski. 2022. Determination of seismic performance factors for cross-laminated timber shear walls vased on FEMA P695 methodology. General Technical Report FPL-GTR-281. US Department of Agriculture, Washington, D.C.

van de Lindt, J. W., J. Furley, M. O. Amini, S. Pei, G. Tamagnone, A. R. Barbosa, D. Rammer, P. Line, M. Fragiacomo, and M.

Popovski. 2019. Experimental seismic behavior of a two-story CLT platform building. *Eng. Struct*. 183:408–422. https://doi.org/10.1016/j.engstruct.2018.12.079

Wang, J. Y., R. Stirling, P. I. Morris, A. Taylor, J. Lloyd, G. Kirker, S. Lebow, M. Mankowski, H. M. Barnes, and J. J. Morrell. 2018. Durability of mass timber structures: A review of the biological risks. *Wood Fiber Sci*. 50(Special):110–127. https://doi.org/10.22382/wfs-2018-045

Yermán, L., J. H. Zhang, M. Xiao, L.-M. Ottenhaus, and J. J. Morrell. 2022. Effect of wetting and fungal degradation on performance of nailed timber connections. *Constr. Build. Mater*. 353. https://doi.org/10.1016/j.conbuildmat.2022.129113